AIAA 99-2274

Validation of the NSTAR Ion Propulsion System on the Deep Space One Mission: Overview and Initial Results*

J. E. Polk, R.Y. Kakuda, J.R. Anderson, J. R. Brophy, V. K. Rawlin, M. J. Patterson, J. Sovey, J. Hamley

Abstract

Deep Space 1 is the first interplanetary spacecraft to use an ion propulsion system for the primary delta-v maneuvers. The purpose of the mission is to validate a number of technologies, including ion propulsion and a high degree of spacecraft autonomy, on a flyby of an asteroid and two comets. The ion propulsion system has operated now for a total of 1791 hours at engine power levels ranging from 0.48 to 1.94 kW and has completed the deterministic thrusting required for an encounter with the asteroid 1992KD in late July, 1999. The system has worked extremely well after an initial grid short was cleared after launch. Operation during this primary mission phase has demonstrated all ion propulsion system and autonomous navigation functions. All propulsion system operating parameters are very close to the expected values with the exception of the thrust at higher power levels, which is about 2 percent lower than calculated values. This paper provides an overview of the system and presents the first flight validation data on an ion propulsion system in interplanetary space.

Introduction

NASA's New Millennium Program (NMP) is designed to flight validate high risk, high payoff technologies that will be required to execute future Earth orbital and Solar System exploration missions. A xenon ion primary propulsion system (IPS) is one of the key technologies being demonstrated on Deep Space 1 (DS1), the first of the New Millenium missions [1]. This spacecraft was launched in October, 1998 and will fly by the asteroid 1992KD in 1999 and, possibly, comets Borrelly and Wilson-Harrington in 2001. The validation objectives of DS1 include demonstrating the functionality and performance of the ion propulsion system in an environment similar to what will be encountered by future users, the compatibility of the IPS with the spacecraft and science instruments, and autonomous navigation and control of the IPS with minimum ground mission operations support. Operation of the propulsion system for the primary mission is now nearly complete. The in-space performance of the propellant feed system is discussed in reference [2] and preliminary results on the interactions of the IPS with the spacecraft and instrumentation are presented in [3]. This paper provides an overview of the DS1 flight system and summarizes the results of validation activities associated with the engine performance and mission operations.

Overview of the NSTAR Ion Propulsion System

The flight ion propulsion system was delivered to DS1 by the NASA Solar Electric Propulsion (SEP) Technology Applications Readiness (NSTAR) program, a joint Jet Propulsion Laboratory/Glenn Research Center effort to develop NASA's 30 cm ion thruster technology for flight applications with industry participation from Hughes Electron Dynamics, Moog, Inc. and Spectrum Astro, Inc. A block diagram of the four major system components is shown in Fig. (1). The ion thruster uses propellant deliv-

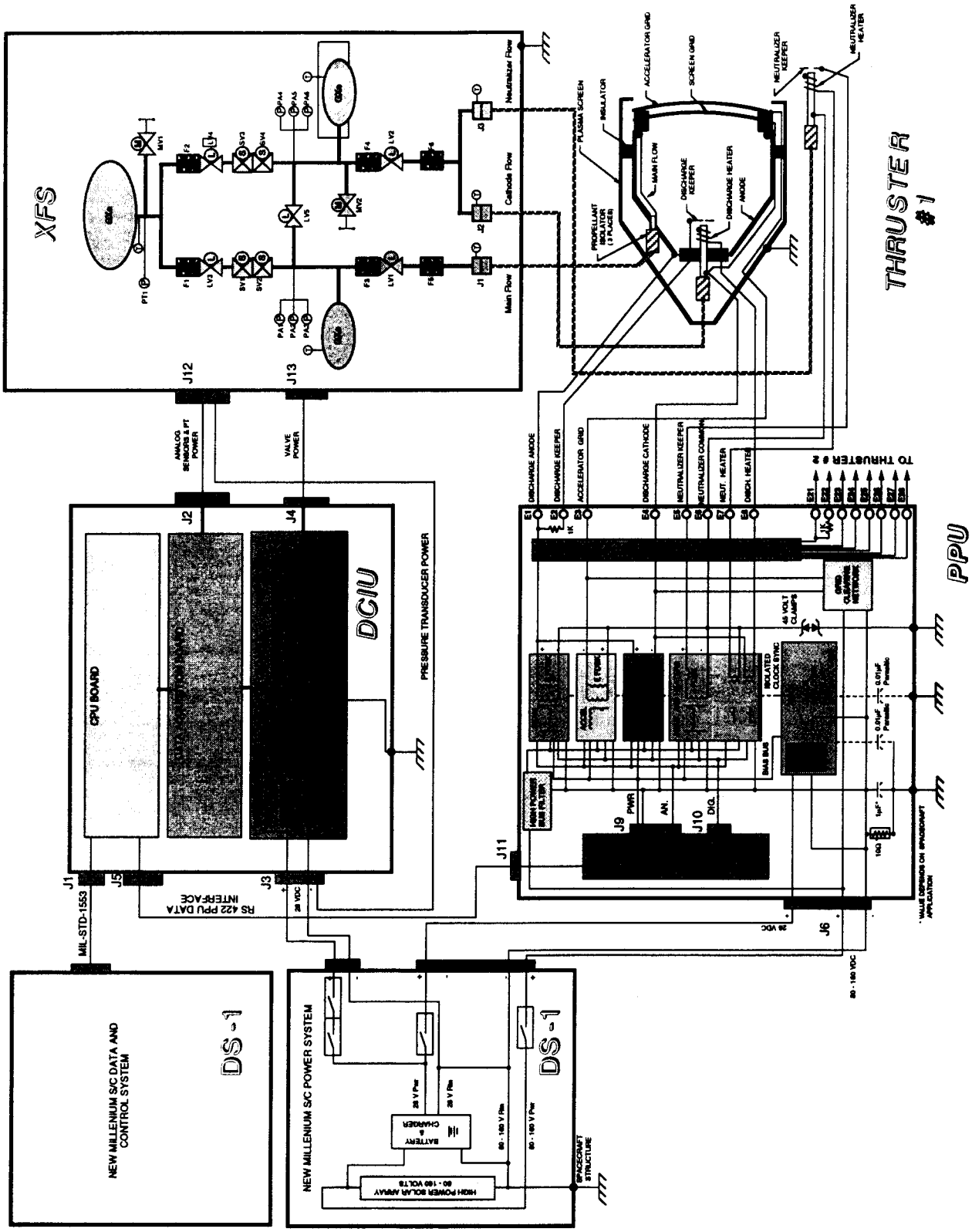

Figure 1: Functional block diagram of the NSTAR ion propulsion system

ered by the Xenon Feed System (XFS) and is powered by the Power Processing Unit (PPU), which converts power from the solar array to the currents and voltages required by the engine. The XFS and PPU are controlled by the Digital Control Interface Unit (DCIU), which accepts and executes high level commands from the spacecraft computer and provides propulsion subsystem telemetry to the spacecraft data system. Planetary missions often require a wide throttling range to accommodate variations in solar array output power with distance from the Sun, so the NSTAR IPS was designed to operate over an engine power range of 500 W to 2300 W. The development of the flight system is discussed in detail in references [4]. The following sections provide a brief summary of the four main system elements.

Ion Thruster

A cutaway view of the 30-cm diameter flight ion thruster fabricated by Hughes Electron Dynamics (HED) is shown in Fig. (2). There are four main components: the discharge chamber, which serves as the anode and the main structural element, the discharge cathode assembly, the neutralizer cathode assembly, and the external plasma screen which is grounded to the spacecraft. This engine is based on technologies developed by NASA [4] and is designed to operate over an input power range of 0.5–2.3 kWe with a thrust of 20–92 mN, a specific impulse of 1950–3100 s and a total beginning-of-life efficiency of 0.42–0.62. The design life is 8000 hours at the full power operating point or a propellant throughput capability of 83 kg and a total impulse capability of 2.65×10^6Ns for an arbitrary throttling profile. The engine was qualified for operation over a temperature range of -93 to 138°C measured on the front mask of the plasma screen. The structural design of all IPS components was based in part on shock and random vibration requirements specified by DS1 [4]. The mass of the flight thruster is listed in Table (1), but does not include the flight cable. Three gimbal brackets serve as the mechanical interface to the spacecraft. Three resistoflex fittings are used to connect the discharge chamber, main cathode and neutralizer cathode feed lines to the XFS. The thruster internal wiring harness is connected to a terminal assembly in the neutralizer housing. All electrical leads connect to the engine at this point, and are packaged in two bundles inside one external cable. This power cable crosses the gimbal interface and terminates in a field joint on the spacecraft. Two flight thrusters were built for the NSTAR program. Flight thruster 1 (FT1) was integrated onto the DS1 spacecraft, while the flight spare engine (FT2) is now being used in a long duration Mission Profile Test (MPT) [5].

Assembly	Mass (kg)
Thruster	8.33
Power Processing Unit	15.03
Digital Control Interface Unit	2.47
Xenon Feed System	20.47
PPU to Thruster Cable	1.70
Total	48.00

Table 1: Masses of the flight ion propulsion system components on the DS1 spacecraft.

Xenon Feed System

The xenon feed system, shown schematically in Fig. (1), is designed to store up to 83 kg of xenon propellant and provide flow rates controlled to within ±3 percent that range from 6 to 24 sccm for the main flow and 2.4 to 3.7 sccm for the cathodes. The XFS has four main elements. Xenon is stored as a supercritical fluid in a propellant tank which is maintained at a temperature of 20°C. The flow rate accuracy and throttleability is achieved by controlling the pressure in two plenum tanks upstream of porous metal plugs which act as fixed flow control devices (FCDs). The pressures in the plena are measured with multiply redundant pressure transducers and controlled with two bang-bang solenoid valve regulators. The main flow is fed from one plenum, while both cathode lines are manifolded into the other. The FCDs for the two cathodes are closely matched, so the discharge cathode and neutralizer flows are approximately equal over the entire throttling range. The flow rate through the FCDs is a function of upstream pressure and temperature, so the plenum pressure is varied to achieve a commanded flow rate and compensate for changes in the FCD temperatures. All of the flow control components are assembled on a single plate which was built by Moog, Inc. This Xenon

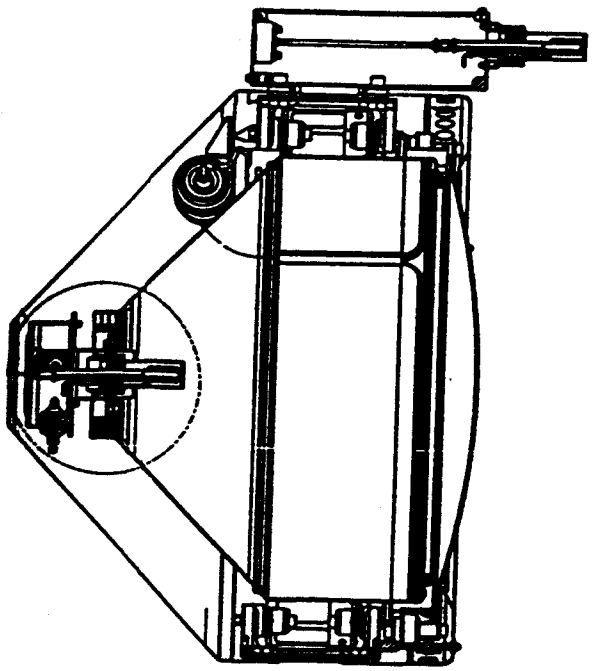

Figure 2: Diagram of the NSTAR ion thruster.

Control Assembly (XCA) was qualified for a temperature range of 20–50°C, and is controlled in flight to a temperature of 25–30°C with heaters. The propellant feed lines exit the xenon control assembly, cross the gimbal mechanism and attach to the thruster with resistoflex fittings. The XCA electrical interfaces include transducer power and analog signals and power to drive the solenoid and latch valves. The mass of the entire flight XFS listed in Table (1) includes tank, flow control components, tubing, wiring and the XCA plate.

Power Processing Unit

The PPU is designed to take an 80–160 VDC input directly from the solar array and supply the appropriate currents and voltages to operate the engine, which are discussed in more detail below. It is packaged in an enclosure which is designed to be bolted onto the spacecraft bus. In addition to the high voltage input bus, the enclosure includes a 28 VDC internal housekeeping bus which provides control power for the internal power supplies and drives an internal "slice" circuit board. This board operates an RS422 command and telemetry interface, digitizes the PPU telemetry and controls the power supplies based on commands from the DCIU. Both input busses have electomagnetic interference filters to meet the conducted emission requirements of MIL-STD-461. The high voltage input is distributed to three inverters operating at 20 kHz which drive the beam, accelerator grid, discharge, neutralizer keeper, discharge cathode heater and neutralizer heater power supplies. The output filters of the discharge and neutralizer keeper supplies consist of an inductor with a pulse-generating winding. Pulses with an amplitude of 650 V and a period of 10 μs are produced on the outputs of these supplies at a 10 Hz rate during thruster ignition to help initiate the discharges. The power supply outputs are routed to internal relays which allow them to be switched to one of two terminal blocks, so that a single PPU can be used to run one of two engines at a time. External power output cables attached to these terminals route power to the field joint on the spacecraft. The PPU was designed to operate with baseplate temperatures between -5 and 50°C with survival temperature limits of -25 and 55°C. On the DS1 mission heater power is required

to meet the lower temperature limits at low output power levels. The flight PPU mass listed in Table (1) includes 1.7 kg for micrometeoroid shielding but the external power cable is listed separately. The PPU was designed with a radiation hardening level of 100 krad.

The PPU contains internal protection for input over-and undervoltage conditions and each supply is short-circuit protected. When a short-circuit is detected on the beam or accelerator grid supplies, internal logic initiates a recycle in an attempt to clear the high voltage fault. The recycle sequence includes turning both supplies off, ramping the discharge current down to 4 A, enabling both supplies again and then ramping the discharge current back to the original setpoint.

Digital Control Interface Unit

The DCIU, built by Spectrum Astro, Inc. serves as the primary data acquisition, control and communications unit in the IPS and is also packaged in a box designed to bolt onto the exterior of the spacecraft. The functions of the DCIU include acquisition, storage and processing of the signals from the sensors on the XFS and telemetry from the PPU slice, control of the valves in the XFS and power supplies in the PPU (through the slice), and communication with the spacecraft data and control system. The DCIU executes stored sequences that control IPS operating modes in response to high level commands generated on the ground or autonomously by the spacecraft. The specific operating modes are discussed in more detail in the next section. The DCIU is powered by the 28 VDC spacecraft auxiliary power bus and contains three half-width VME boards that perform the data acquisition, communications and processing and valve driver functions. The communications with the PPU slice occur over an RS422 interface and commands from and telemetry to the spacecraft are transmitted on a MIL-STD-1553 interface. The DCIU provides power for the valve drivers and transducers in the XFS and recieves analog signals from the sensors. The unit is radiation shielded to 100 krad and is designed to operate from -15 to 50°C with survival limits of -25 to 55°C. The DCIU mass shown in Table (1) does not include the weight of additional thermal control hardware mounted by the DS1 program.

The flight electrical telemetry is calibrated to within ±2 percent of reading for the high voltage supply parameters and ±2 percent of full scale for the other parameters. In this paper the values have been corrected using the ground calibration data and are more accurate–typically the standard error is under 0.2–0.8 percent of full scale. The voltage measurements have also been corrected for flight cable line drops and represent the values that would be measured at the engine

Operating Modes

The DCIU software is designed to perform the functions described briefly in this section. The system also has a number of fault recovery functions which are defined in [6]. Only a few of those will be discussed here.

Cathode Conditioning. After launch the cathodes are heated for 3 hours at 3.85 A and for 1 hour at 7.2 A to help drive off oxidizing impurities from the inserts. This sequence is initiated by a single command and controlled by the DCIU.

Thruster Ignition. This operating mode begins with pressurizing the plenum tanks to the proper values, starting propellant flow to the engine, and preheating the cathodes at 8.5 A prior to ignition of the neutralizer discharge at 2 A. After 210 s of heating, the neutralizer high voltage pulse ignitor is started. After neutralizer keeper current is detected, the heater and ignitors are turned off and the discharge is ignited at 4 A. When both discharges have successfully lit, the high voltage is turned on at the minimum power level and the engine is throttled to the final setpoint. The accelerator grid voltage is set to -250 V for two hours after ignition, then is increased to the final throttle point value.

Steady State Operation. The DCIU is capable of operating the thruster at any one of 16 discrete throttle levels from a throttling table stored in memory. This table contains the setpoints for the PPU power supplies and the XFS pressures and can be modified by ground command. The NSTAR 16 level throttle table showing the entire range of operation is listed in Table (2). The DCIU commands the PPU power supplies to deliver these values and controls the XFS valves to maintain the desired pressures in steady state operation. The beam current setpoint is maintained by

NSTAR Throttle Level	Mission Throttle Level	Beam Supply Voltage (V)	Beam Supply Current (A)	Accelerator Grid Voltage (V)	Neutralizer Keeper Current (A)	Main Plenum Pressure (psia)	Cathode Plenum Pressure (psia)
15	111	1100	1.76	-180	1.5	87.55	50.21
14	104	1100	1.67	-180	1.5	84.72	47.50
13	97	1100	1.58	-180	1.5	81.85	45.18
12	90	1100	1.49	-180	1.5	79.29	43.80
11	83	1100	1.40	-180	1.5	76.06	42.38
10	76	1100	1.30	-180	1.5	72.90	41.03
9	69	1100	1.20	-180	1.5	69.80	40.26
8	62	1100	1.10	-180	1.5	65.75	40.26
7	55	1100	1.00	-150	2.0	61.70	40.26
6	48	1100	0.91	-150	2.0	57.31	40.26
5	41	1100	0.81	-150	2.0	52.86	40.26
4	34	1100	0.71	-150	2.0	48.08	40.26
3	27	1100	0.61	-150	2.0	43.18	40.26
2	20	1100	0.52	-150	2.0	39.22	40.26
1	13	850	0.53	-150	2.0	39.41	40.26
0	6	650	0.51	-150	2.0	40.01	40.26

Table 2: Flight throttle table of parameters controlled by the DCIU

closed-loop control of the discharge current.

Throttling. When a new throttle level is commanded, the DCIU ramps the XFS pressures and PPU outputs to the new values. If the power level is being increased, the flows are raised before the engine power is changed. To throttle down, the electrical parameters are changed first, then the flow rates.

Thruster Power Down. In this operating mode the power supplies are turned off and all XFS valves are closed.

Continuous Recycling Fault Mode. The DCIU monitors the number of recycle events initiated by the PPU under high voltage fault conditions. If 25 or more are recorded in a 90 s time period, the engine is shut off and a fault flag is set.

Grid Clear Fault Recovery. In the event of a physical short between the grids that cannot be cleared by recycling or mechanical methods, the DCIU can be commanded to execute a grid clear operation. In this operating mode, internal relays in the PPU are closed to apply the discharge supply to the ion optics. The supply is then turned on at 4 A for a period of 30 s in an attempt to resistively heat and vaporize the short.

These DCIU functions can be called with ground commands. In addition, the spacecraft can generate commands to the IPS to perform certain operations. The IPS is throttled autonomously by the spacecraft to track the solar array output. DS1 also includes an autonomous system (AutoNav) to navigate the spacecraft to the next encounter target. This system contains an optimized trajectory that was computed on the ground and a catolog of ephemerides for a number of stars, asteroids, the planets and the DS1 target bodies. Periodically (one to three times per week) during a burn, the system automatically turns the spacecraft to optically observe the positions of a number of these bodies against the stellar background and calculates the spacecraft position. The heliocentric orbit is then determined and the trajectory propogated to the next target. Required course changes are generated by the maneuver design element and accomplished by varying the IPS thrust direction and duration. This technology dramatically reduces the need for mission operations support, as described below.

The NSTAR Throttle Table

The NSTAR 16 point throttle table contains the IPS setpoints required to operate the system over the required throttling range. A corresponding mission throttle table containing the flow rates, thrust and PPU input and output power levels is required to

NSTAR Throttle Level	Mission Throttle Level	PPU Input Power (kW)	Engine Input Power (kW)	Calculated Thrust (mN)	Main Flow Rate (sccm)	Cathode Flow Rate (sccm)	Neutralizer Flow Rate (sccm)	Specific Impulse (s)	Total Efficiency
15	111	2.52	2.29	92.4	23.13	3.70	3.59	3120	0.618
14	104	2.38	2.17	87.6	22.19	3.35	3.25	3157	0.624
13	97	2.25	2.06	82.9	20.95	3.06	2.97	3185	0.630
12	90	2.11	1.94	78.2	19.86	2.89	2.80	3174	0.628
11	83	1.98	1.82	73.4	18.51	2.72	2.64	3189	0.631
10	76	1.84	1.70	68.2	17.22	2.56	2.48	3177	0.626
9	69	1.70	1.57	63.0	15.98	2.47	2.39	3136	0.618
8	62	1.56	1.44	57.8	14.41	2.47	2.39	3109	0.611
7	55	1.44	1.33	52.5	12.90	2.47	2.39	3067	0.596
6	48	1.32	1.21	47.7	11.33	2.47	2.39	3058	0.590
5	41	1.19	1.09	42.5	9.82	2.47	2.39	3002	0.574
4	34	1.06	0.97	37.2	8.30	2.47	2.39	2935	0.554
3	27	0.93	0.85	32.0	6.85	2.47	2.39	2836	0.527
2	20	0.81	0.74	27.4	5.77	2.47	2.39	2671	0.487
1	13	0.67	0.60	24.5	5.82	2.47	2.39	2376	0.472
0	6	0.53	0.47	20.6	5.98	2.47	2.39	1972	0.420

Table 3: Flight throttle table of parameters used in mission analysis.

perform the mission trajectory design. The NSTAR mission table is listed in Table (3). The development of these throttle tables is described in this section.

Power throttling is accomplished by varying the beam voltage and current. The engine throttling envelope with lines of constant beam power is shown in Fig. (3). The boundaries of this envelope represent the maximum beam voltage and current capabilities, the minimum beam current (which is determined primarily by the minimum discharge current) and the beam voltage perveance limit. The NSTAR throttle table was designed to maximize the specific impulse, so the power is varied with beam current throttling over most of the range. The lowest power levels are achieved by operating at the minimum beam current and throttling the beam voltage.

The discharge chamber flow rate was selected to give the propellant utilization shown in Fig. (4). The propellant efficiency of 0.9 was selected at high power levels as a compromise between maximizing total engine efficiency and minimizing double ion production, which can drive internal erosion rates. A propellant efficiency of 0.9–0.91 is maintained over most of the range. At the lowest powers the double-to-single ion current ratio is low, so the propellant efficiency was chosen to give a discharge loss that yielded the correct total power at that point.

The neutralizer and cathode flow rates are approximately equal at each operating point and vary over the throttling range as shown in Fig. (5). The minimum flow rate was designed to prevent the neutralizer from operating in plume mode, which can cause excessive erosion of the orifice. End-of-life neutralizer characterization data from the 8200 hour Life Demonstration Test (LDT) of an engineering model thruster (EMT2) are shown on this plot as well [7]. The maximum flow rate was chosen to match the discharge cathode flow rate used in a 1000 hour test of an engineering model thruster which demonstrated little cathode erosion compared to a previous 2000 hour test at a lower flow rate [8]. Subsequent tests suggest that other design changes were responsible for the erosion rate reduction, but the higher flow was maintained to be conservative.

The thrust in the mission throttle table is calculated from the engine electrical setpoints,

$$T = \alpha F_t J_b (V_s - V_g)^{1/2} \left(\frac{2M}{e}\right)^{1/2} \qquad (1)$$

where J_b is the beam current, V_s is the beam power supply voltage, V_g is the coupling voltage between neutralizer common and the facility ground or ambient space plasma, M is the mass of a xenon ion and e is the charge of an electron. The factors α and F_t cor-

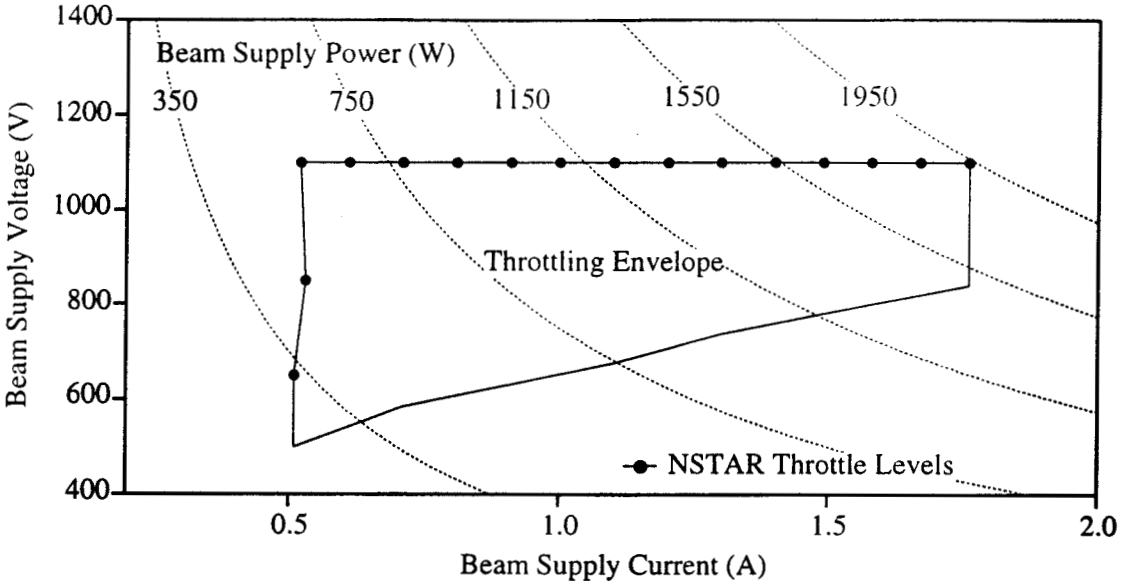

Figure 3: NSTAR power throttling strategy.

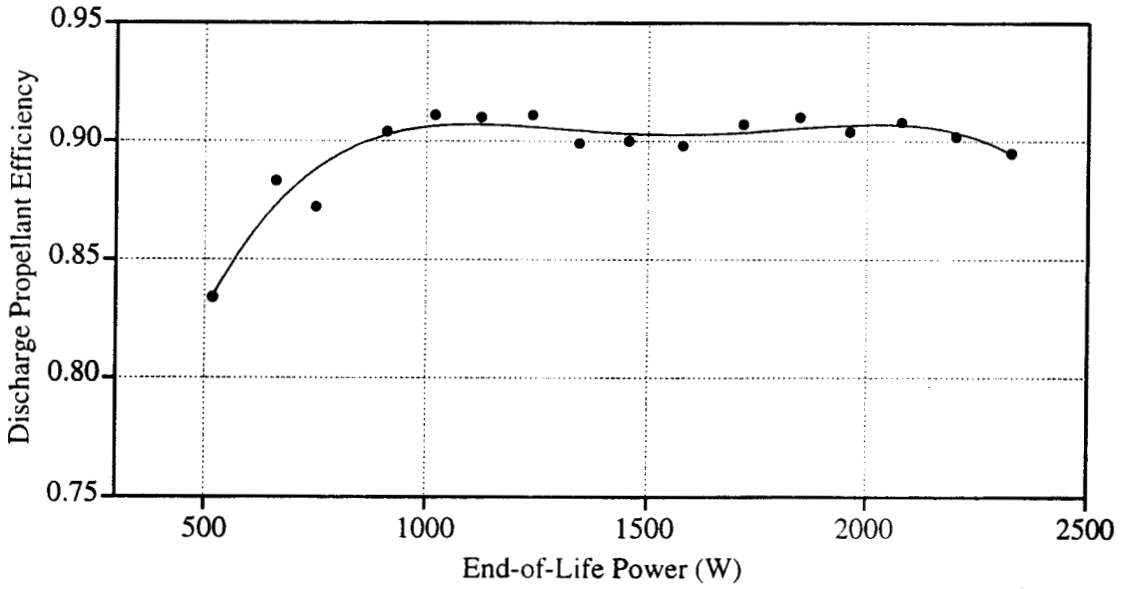

Figure 4: NSTAR ion thruster discharge propellant utilization efficiency.

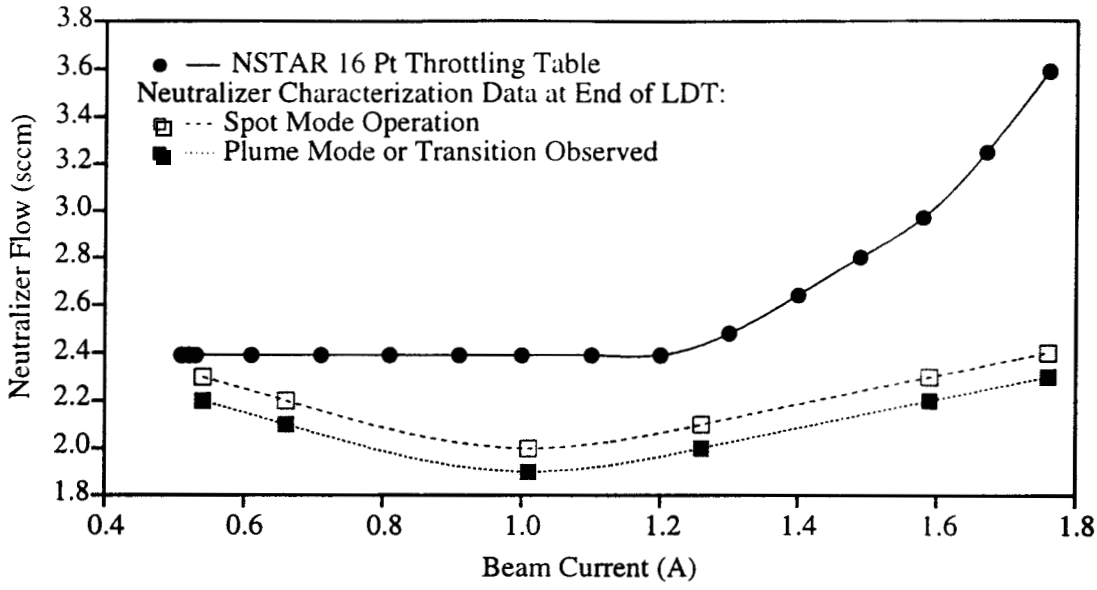

Figure 5: NSTAR cathode flow rates.

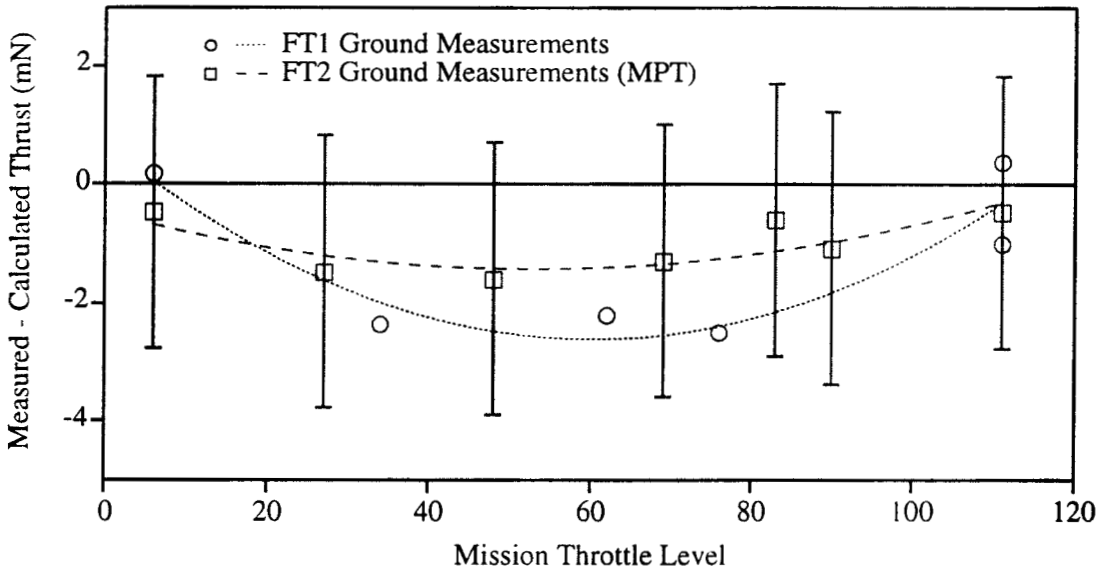

Figure 6: The difference between measured and calculated thrust over the NSTAR throttling range.

rect for the doubly-charged ion content of the beam and thrust loss due to non-axial ion velocities [9]. A constant value of 0.98 for F_t based on earlier 30-cm thruster ground tests and a value of α based on a curve fit to centerline double ion current measurements as a function of propellant utilization efficiency in a 30 cm, ring-cusp inert gas thruster[10] were used. Earlier direct measurements of thrust from the LDT agreed well with the calculated value [9, 7]. More recent measurements with the flight thrusters were somewhat lower than the calculated values for intermediate throttle levels. The difference between the measured thrust and the table values is shown in Fig. (6).

The power required for a given thrust level increases over the engine lifetime due to wear [9], so two tables representing beginning-of-life (BOL) and end-of-life (EOL) were developed. These have the same engine setpoints shown in Table (2) but different engine power levels. The BOL table was developed primarily through testing with engineering model thrusters and updated with data from preflight measurements with FT1. The EOL table was based largely on measurements from the 8200 hour test of EMT2. The power at the lowest throttle levels was extrapolated from performance curves obtained after about 6500 hours of operation. The extrapolations were based on sensitivity data, which were used to correct for slight differences in some of the controlled parameters. The difference between BOL and EOL engine power is plotted in Fig. (7). Additional measurements taken at some of these throttle levels after about 6900 hours of operation in the LDT are also shown. They suggest that the EOL power at some of the lower throttle levels is overestimated in the throttling table. BOL data obtained with the two flight thrusters demonstrates that their initial performance agrees well with the table values.

The PPU input power corresponding to a given engine power is determined by the PPU efficiency. The efficiency of the flight PPU was characterized as a function of input bus voltage and temperature in several ground tests, as shown in Fig. (8). The lowest measured values over this range of parameters were used to define the lowermost line in the figure. This conservative estimate of PPU efficiency was used to generate the PPU input powers in the throttle table.

In order to make finer steps in power throttling to more closely track the solar array peak power, a 112 point throttle table was also developed for use in flight. Power throttling between the 16 NSTAR throttle points is accomplished by varying the beam voltage to give steps that are approximately 20 W apart. A 16 point subset of this table is loaded into the DCIU to provide fine throttle control over a restricted power range for a given mission phase.

Post-Launch IPS Operation and Validation Activities

Operation of the ion propulsion system during the DS1 primary mission can be organized into several phases. These phases are summarized in this section.

Decontamination

The first IPS in-space activity was a bakeout of the downstream portion of the propellant feed system that occurred six days after launch. Prior to this the thruster axis was oriented 90° away from the Sun and the thruster front mask temperature was -45°C. The spacecraft was turned so that the angle between the axis and the Sun was 30° to warm the thruster and feed system. Over a 29 hour period the thruster temperature exceeded 110°C and the XFS lines reached over 45°C. This was done to help remove any residual contaminants in the portions of the feed system that had been exposed to air prior to launch. The cathode conditioning sequence was then executed to bakeout the cathode inserts. Finally, 16 days after launch, the discharges were operated for four hours at high power levels to further bakeout the engine prior to application of high voltage.

Initial Start and Grid Short

The following day the first engine ignition occurred. Both cathodes lit properly and the engine ran nominally at the minimum power point for 4.5 minutes before continuous recycling caused a thruster shutdown. A short between the grids was suspected, but at this point a failure of one of the high voltage supplies could not be ruled out. Fourteen additional start attempts were made under various engine thermal conditions (created by spacecraft turns toward or away from the Sun), but all ended in continuous recycling when the high voltage was applied.

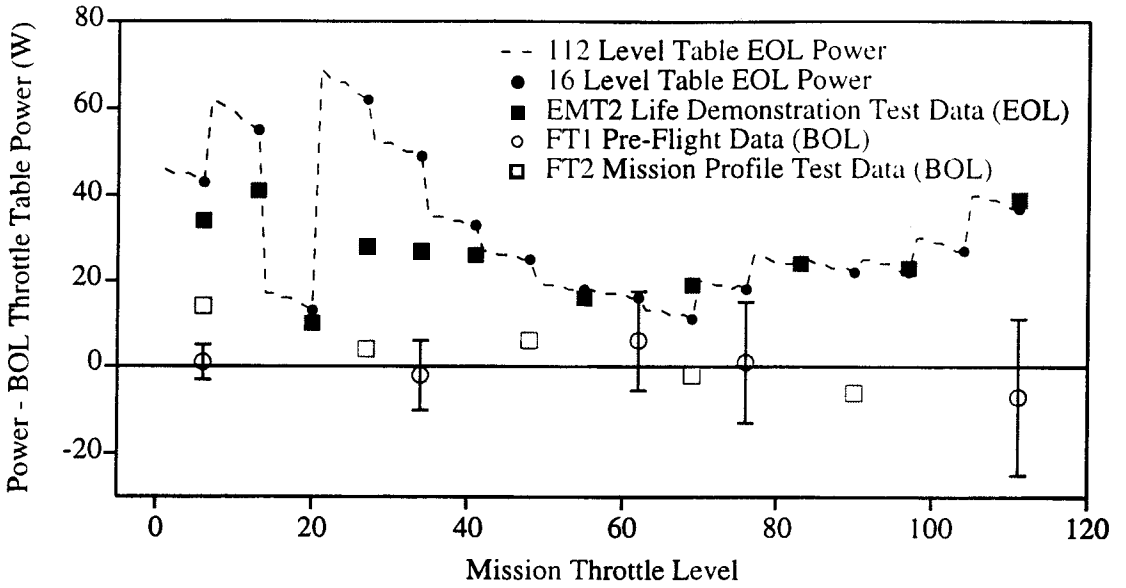

Figure 7: Difference between a given power level and the beginning-of-life power.

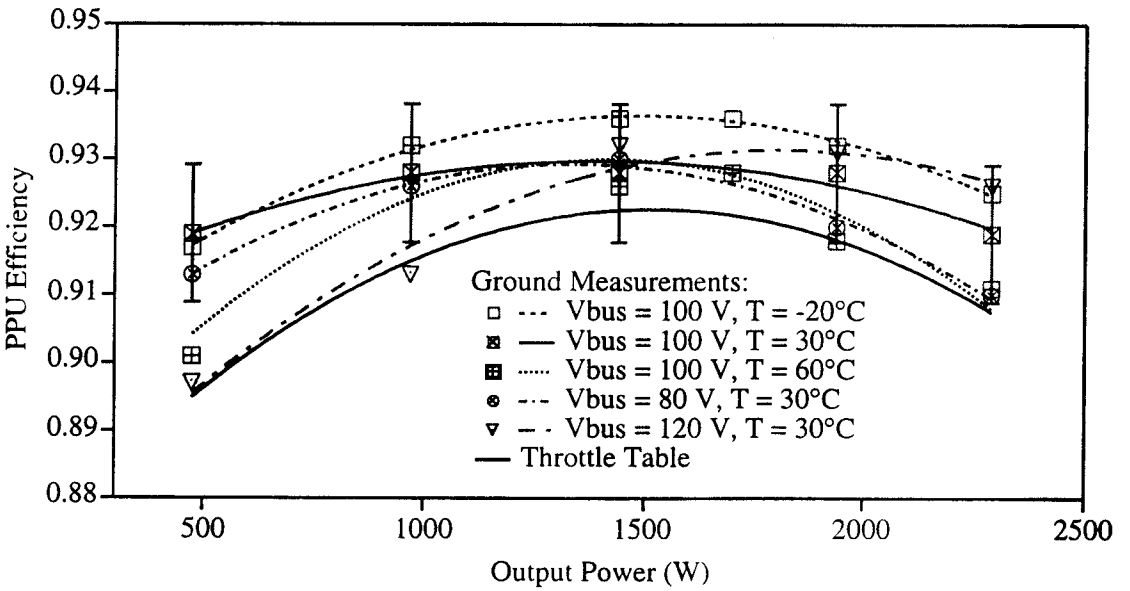

Figure 8: PPU efficiency measurements.

Troubleshooting

Delta-v maneuvers using the IPS were not required to encounter the target bodies until much later in the mission, so a detailed investigation of the problem was undertaken. Several options were identified, including attempting a grid clear command, thermally cycling the engine to force a mechanical separation of the grids that might dislodge a particle, running additional recycles and developing additional diagnostics to help identify the fault.

The NSTAR PPU is designed to deliver 4 A into a grid short to clear those that are not cleared by recycles, as outlined above. However, this system was designed primarily to clear thin molybdenum flakes generated by spalling of sputter-deposited films inside the discharge chamber after many thousands of hours of operation. Grid shorting this early in a mission was more likely due to particulates from the launch vehicle payload fairing or generated during the payload separation, which could be much larger than films from the discharge chamber. The risk of permanently welding a large particulate between the grids with the standard grid clear circuit was not known, so an experimental and theoretical effort to characterize the grid clear process was undertaken prior to using it under these circumstances. The results of this investigation are reported in [11].

Thermal and structural models of the ion optics were also coupled during this period to determine the mechanical effect of thermally cycling the grids. This modeling showed that significant transient changes in the grid spacing can be achieved by turning the spacecraft to heat or cool the grids. This technique was used to clear grid shorts on the SERT II flight experiment [12] and appeared to have the least risk. During the two week problem investigation period the spacecraft was turned several times to thermally cycle the grids.

The IPS is designed with hardware interlocks which prevent operation of the high voltage supplies before the discharges are ignited, so it was not possible to command these supplies on separately to test them. The DCIU software was modified to provide brief bursts of high speed data for various PPU electrical parameters during recycles to help diagnose which supplies were affected. Finally, a test involving operation of the discharge supply only with no flows (which is allowed by the system) was developed. If the grids are shorted, the accelerator grid voltage telemetry will change when the discharge open circuit voltage is applied, otherwise it remains close to zero. This is a clear discriminator between open circuits and shorts on the ion optics.

Recovery Start

Thirty one days after launch the discharge-only test was executed and the results suggested that the grids were not shorted. Another start attempt was then made, primarily with the intent to gather high speed engine data during continuous recycling to help diagnose the fault. Fortunately the engine started properly this time, and has continued to run flawlessly since this point. Apparently the thermal cycling successfully cleared debris lodged between the grids.

First Performance Test

Over the next 335 hours the engine was operated at power levels ranging from 0.48 to 1.94 kW to characterize the BOL performance. This burn was used to contribute to the required spacecraft delta-v, but was not controlled by AutoNav. The throttle levels were dictated primarily by the validation objectives. This test was designated IPS Acceptance Test 1 (IAT1).

Deterministic Thrusting

IAT1 was followed by 95 hours of thrusting at power levels ranging from 1.7 to 1.86 kW. These initial operations also contributed to the required total impulse, but were executed with ground commands. These were followed by a coast period of 74 days, then seven navigational burns (NBURNs) totalling 912 hours of operation. These maneuvers were executed autonomously by AutoNav and used automatic peak power tracking to determine the maximum achievable throttle level. The first of these, NBURN 0, did not use the optical navigation for spacecraft position determination, but all subsequent NBURNs have exercised the full AutoNav capability. This portion of the mission is on an outbound portion of the trajectory, so the available array power has dropped continuously. NBURN 0 was run with engine power levels ranging from 1.73 to 1.62 kW, while the following six

were performed with power levels of 1.18 to 0.71 kW. These burns completed the deterministic thrusting required for the encounter with asteroid 1992KD.

Second Performance Test

After another coast period of 21 days a second throttling test was performed. This brief test, designated IAT2, was restricted to power levels ranging from .49 to .98 kW by total solar array power.

Trajectory Correction Maneuvers

In addition to the deterministic burns, the IPS will be used for some of the final trajectory correction maneuvers (TCMs) prior to the asteroid encounter. These burns will each last about 25 hours and will place the spacecraft on a trajectory which will pass within 10 km of the asteroid. TCMs on the final day before the encounter will be performed with the hydrazine attitude control thrusters. Certain spacecraft attitudes with respect to the Sun are not allowed because of the orientation of sensitive optical instruments or thermal control surfaces. If thrust is required in a direction disallowed by these constraints, the maneuver will be decomposed into two burns in safe directions with a resultant thrust in the proper direction. All of these operations will be executed by AutoNav with no ground intervention.

In-Flight System Performance

One of the primary objectives of the flight validation activity is to verify that the system performs in space as it does on the ground. The parameters of interest to future mission planners are those in the mission throttle table: thrust and mass flow rate as a function of PPU input power. In this section the system power, thrust and mass flow rate behavior will be evaluated in terms of the throttle table.

PPU Power Input Requirements

The PPU input power is determined by the PPU output power (engine power requirement) and the PPU efficiency. The difference between the in-flight engine input power and the BOL throttle table power is shown in Fig. (9). These power values are based on the individual power supply current and voltage telemetry readings. The total engine power consumed during the IAT1 throttle test and initial operations differed from the table values by only about 2 W on average, although the uncertainties are much larger than this, as shown by representative error bars on the figure. The engine power requirement increased by 12–15 W with time, however, as the data from NBURNs 1–3 and IAT2 show. This is a normal consequence of engine aging [9, 7], and the total power at this point in the mission is still less than the EOL power used in the throttle table, which is represented by the solid line in Fig. (9). This increased power demand is due primarily to increased discharge power losses, as discussed in the next section.

In-flight measurements of the PPU efficiency suggest that it is higher than that measured in ground tests, as shown in Fig. (10). These values are based on the total engine power and PPU high voltage bus current and voltage telemetry with an additional 15 W assumed for the low voltage bus input power. There is no telemetry for the low voltage bus, but ground testing showed a 15 W loss for all conditions. The efficiency is sensitive to the line voltage and the temperature, as the ground data show. The in-flight measurements were taken with line voltages of 95 ± 5 V and baseplate temperatures ranging from 0 to 37°C, so they should be compared with the solid line in the center of the pre-flight data and the highest dashed line. The range of uncertainty in these measurements encompasses the ground test data, but the in-space measurements appear to be higher systematically by about 1 percentage point. This apparent performance gain is not understood and may be due to a systematic error in the ground or flight measurements.

If the PPU efficiency is actually higher than anticipated, it more than offsets the increased output power requirements observed so far in the primary mission. Figure (11) displays the difference between the observed PPU input power and the BOL input power from the throttle table. The input power required early in the mission was approximatly 20 W lower than expected, because of the higher PPU efficiency. The data from the NBURNs and IAT2 show that the input power is just now approaching the BOL throttle table value.

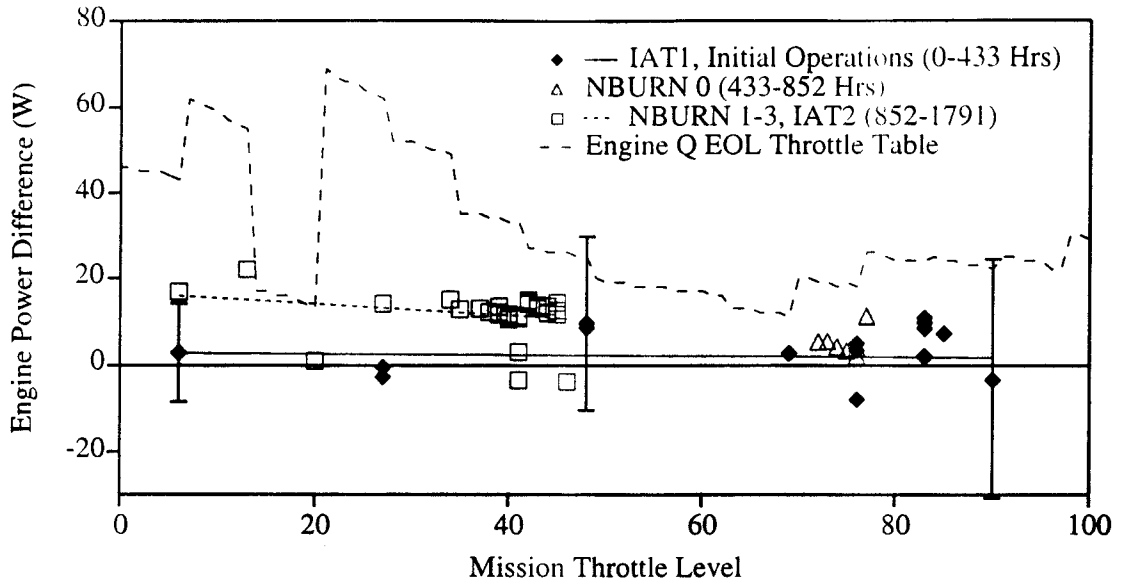

Figure 9: Difference between a given power level and the throttle table BOL values.

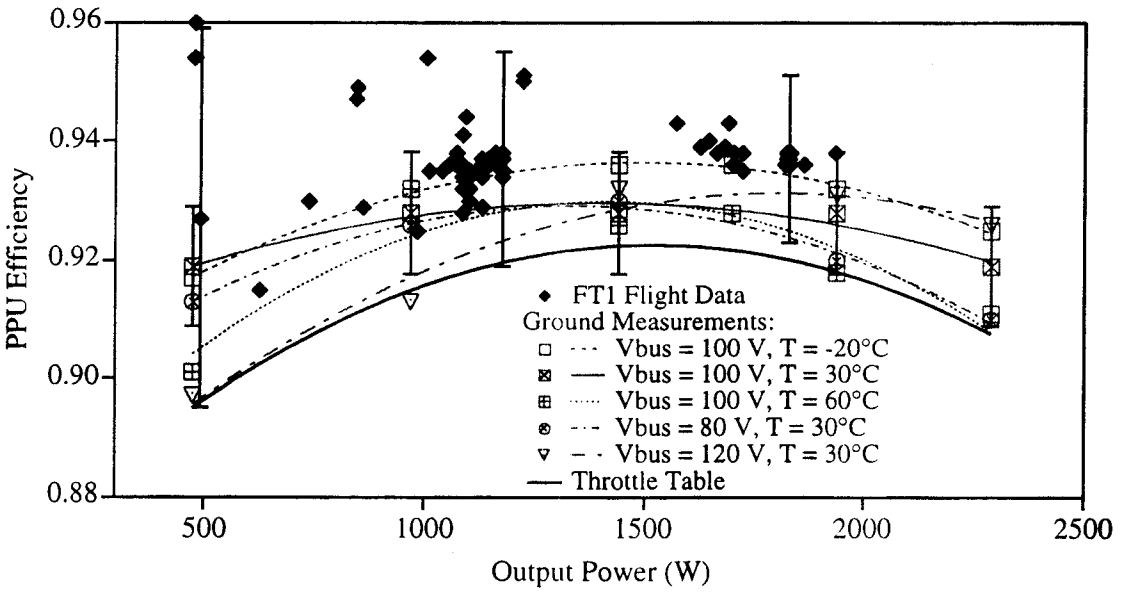

Figure 10: In-flight measurements of PPU efficiency compared to ground test data.

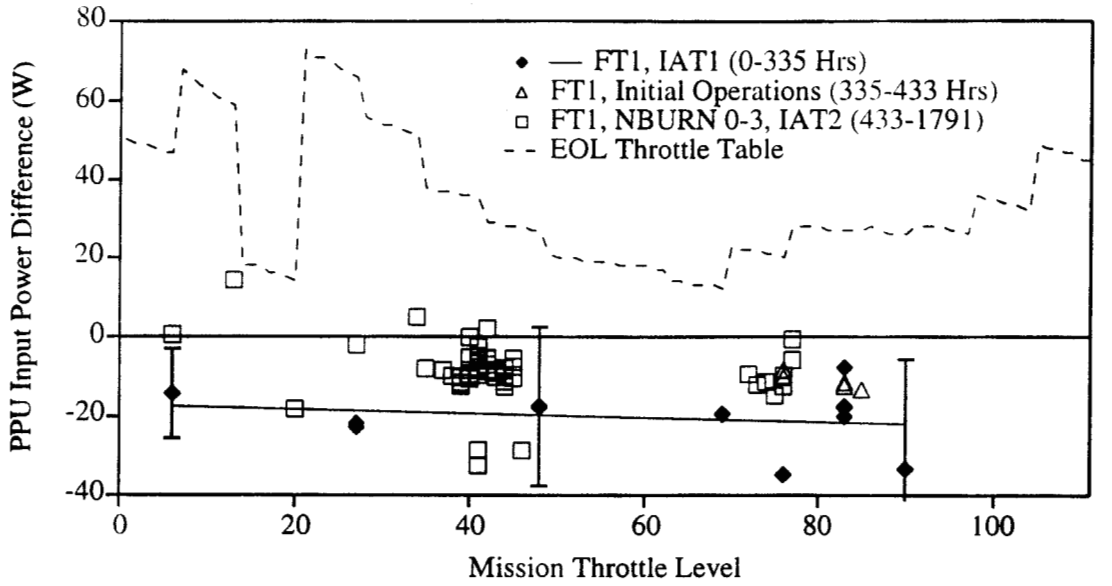

Figure 11: Difference between a given PPU input power level and the corresponding throttle table BOL value.

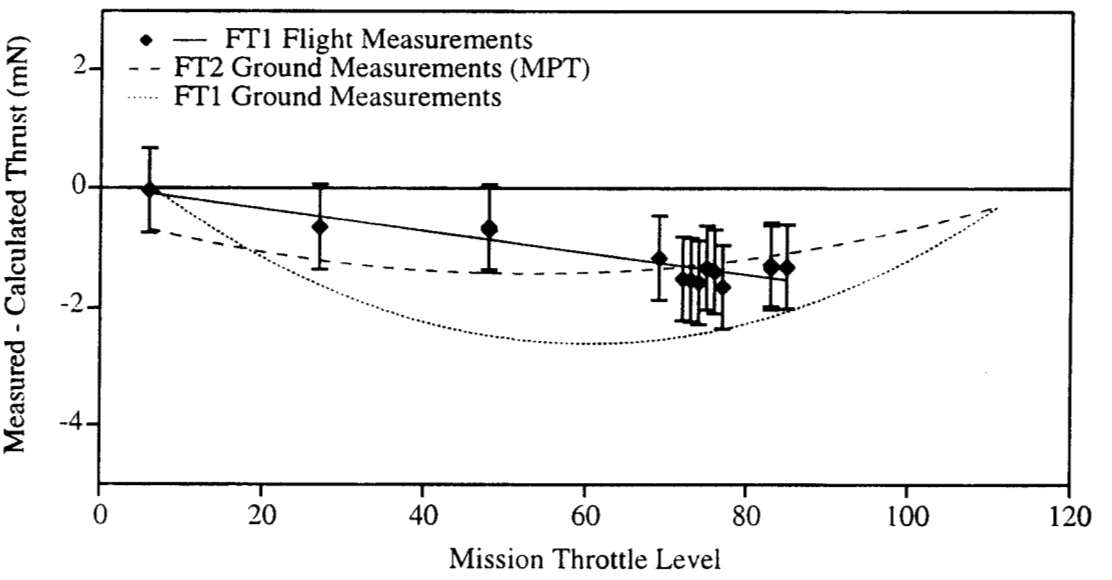

Figure 12: Difference between measured and calculated thrust in flight compared to ground measurements.

IPS Thrust

The acceleration of the spacecraft is measured very accurately from changes in the Doppler shift of the telecommunications signals. With models of the spacecraft mass as a function of time, the Doppler residual data can be used to measure the thrust of the IPS with an uncertainty of less than 0.5 mN. Preliminary thrust measurements have been obtained so far from IAT1, the initial operations and NBURN 0. The flight beam voltage and current values, which determine to a large extent what the thrust is, are slightly different from the setpoints in the table. The flight thrust measurements are therefore compared to the thrust calculated from the actual electrical parameters rather than the table values. The difference in the measured and calculated thrust is shown in Fig. (12), with the curve fits to similar data obtained with a thrust balance in ground tests. The ground and flight data agree well with the calculated values at low power levels, but are lower at intermediate powers. The flight data suggest that the difference in true thrust and calculated thrust grows linearly with power, peaking at 1.6 mN lower than expected at mission level 83 (1.82 kWe engine power). The error bars shown in this figure are based on the uncertainty in the measured thrust and do not include errors in the calculated thrust.

This discrepancy may also be due to a systematic error in the flight telemetry, although the agreement with ground data argues against that conclusion. As Eq. (1) shows, the true thrust might be lower than calculated because of a higher double ion content, greater beam divergence than observed in the previous 30-cm thruster tests or differences in the coupling voltage in-space compared to ground tests. Additional measurements and analysis will be required to resolve this issue.

Although the actual thrust appears to be slightly lower than expected, at the beginning of the mission the overall system performance was still very close to the BOL throttle table level, in terms of thrust for a given PPU input power. Figure (13) shows that at the beginning of the mission the higher PPU efficiency largely compensated for the lower thrust. In this comparison, the thrust is within 0.5 mN of the table values. The gap between the two widens as the engine wears and the total engine power requirement for a given throttle level grows, however. The PPU input power required for the thrust levels measured during NBURN 0 has exceeded the EOL throttle table power for an equivalent thrust.

The thrust vector behavior in-flight is similar to that observed in ground tests. The engine is mounted on a two-axis gimbal with range of ±5°. When the IPS is not operating, a hydrazine attitude control system is used for 3-axis stabilization. After ignition of the ion thruster, control in two axes is transferred to the IPS gimbal system. Potentiometers on each axis of the gimbal provide a measure of the thrust vector stability during IPS operation. There is a brief transient after transfer of control, but after that the mean value of the gimbal angle appears to be stable over long periods of time. The thrust vector of the flight engine relative to the thruster axis was measured using a thrust vector probe [13] prior to integration and alignment on the spacecraft. The gimbal angle data in Fig. (14) show that this alignment was excellent. They also demonstrate that the thrust vector changes slightly with throttle level, as shown in previous ground tests [13].

Propellant Flow Rates

The performance of the xenon feed system is discussed in detail in [2]. In general, the performance has been excellent, although the flow rates are slightly higher than the throttle table values. The mean value of the main flow is 0.05–0.14 sccm (about 0.4 to 1.0 percent) high, while that of the two cathode flows is 0.03 sccm (about 1.0 percent) high. This is in part intentional. As Fig. (15) shows, the XFS bang-bang regulators result in a sawtooth pressure profile. The control system is designed so that the minimum pressure in this sawtooth yields the throttle table flow rate values. In addition to this deliberate conservatism, there is a slight bias in both regulators because one of each of the three pressure transducers on the two plena had a slight offset after launch.

Overall System Performance

The propulsion system performance can be summarized in terms of specific impulse and efficiency. At the beginning of the mission the Isp was about 60 s lower than expected and the engine efficiency was 2

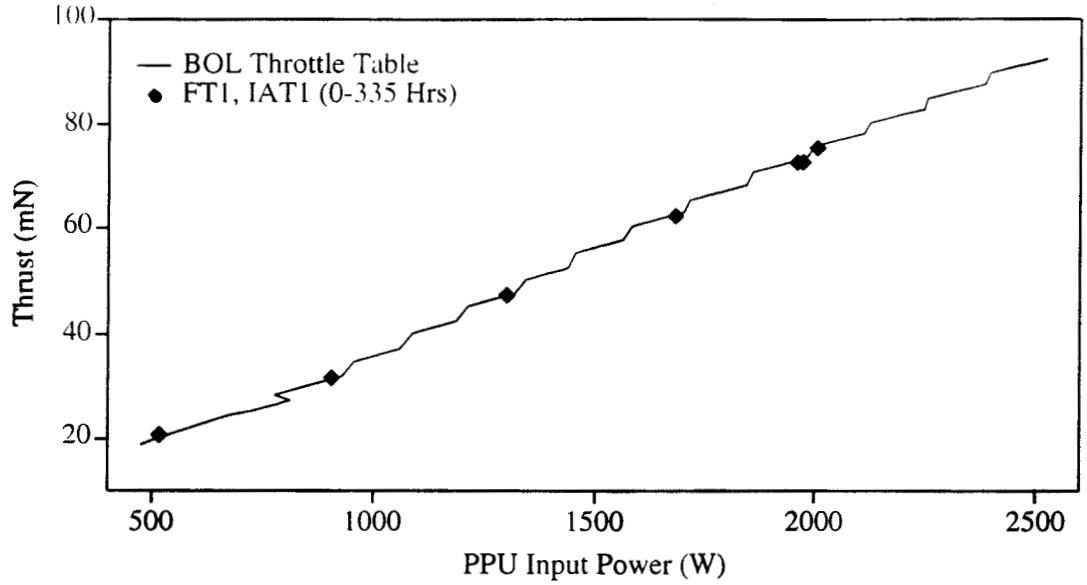

Figure 13: Measured thrust as a function of PPU input power compared to throttle table values.

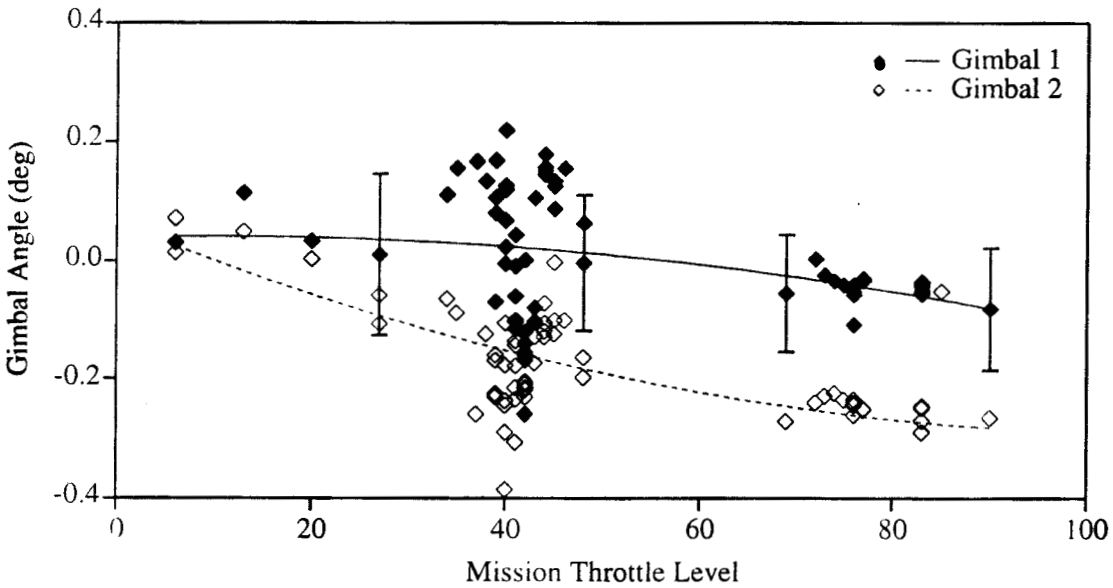

Figure 14: Gimbal positions as a function of mission throttle level.

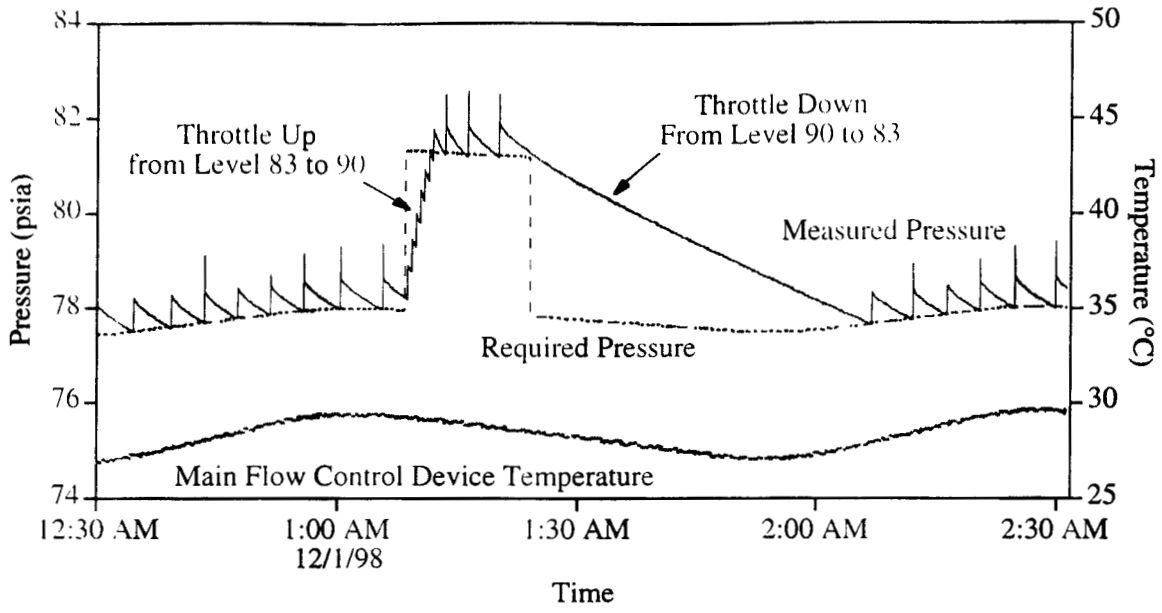

Figure 15: Example of flow rate throttling.

to 2.5 percentage points lower than the throttle table values. The measured performance was still excellent, with a measured efficiency of 0.42 to 0.60 at Isp's ranging from 1960 to 3125 s over an engine throttling range of 478 to 1935 W. The measured mission planning performance parameters are summarized in Table (4).

Engine Behavior In-Flight

The engine behavior in space has been very similar to that observed in ground testing. The detailed operating characteristics of the engine are discussed in this section.

Engine Ignitions

A total of 32 successful engine ignitions have occurred in the first 1791 hours of the primary mission with only one failure to achieve beam extraction due to the initial grid short discussed above. The data from the first 25 ignitions are reviewed here. The nominal heater current value is 8.5 A; the actual cathode and neutralizer heater currents in-flight have been constant at 8.414 A and 8.375 A, respectively. The time history of the heater voltages, which are an indicator of heater health, are plotted in Fig. (16). The uncertainty in these measurements is about ± 2 percent. The first 15 ignitions include the first successful engine start and 14 start attempts after continuous recycling shut the thruster off. The peak heater voltage is a function of the heater impedence, current and temperature. The data show that the heater voltage increases in any rapid sequence of ignitions because the conductor is hotter at the beginning of each consecutive start. The subsequent data show that the heater voltage is also higher when the initial thruster temperature (indicated by the front mask temperature in the plot) is higher. The scatter in the peak voltages under similar temperature conditions is low and very similar to that observed in ground tests.

The time required for the cathodes to ignite after the 210 s heat phase and application of the high voltage ignitor pulses is plotted in Fig. (17). The neutralizer ignition delays show trends which also follow initial temperature, with 20–80 s delays observed for the lowest temperatures. Delays of up to 86 s were also observed during ground thermal tests at the lowest temperatures [14], and are not considered to be a concern. In all cases the discharge cathode has ignited 5–6 s after successful neutralizer ignition, which reflects delays in the start sequence. Its ignition reliability may be higher because it has a slightly higher heater current and because it automatically goes through a longer heat phase when the neutralizer ignition is delayed.

Throttling Characteristics

The throttling sequences were in all cases executed properly by the DCIU after receiving ground commands. An example of the throttling sequence is

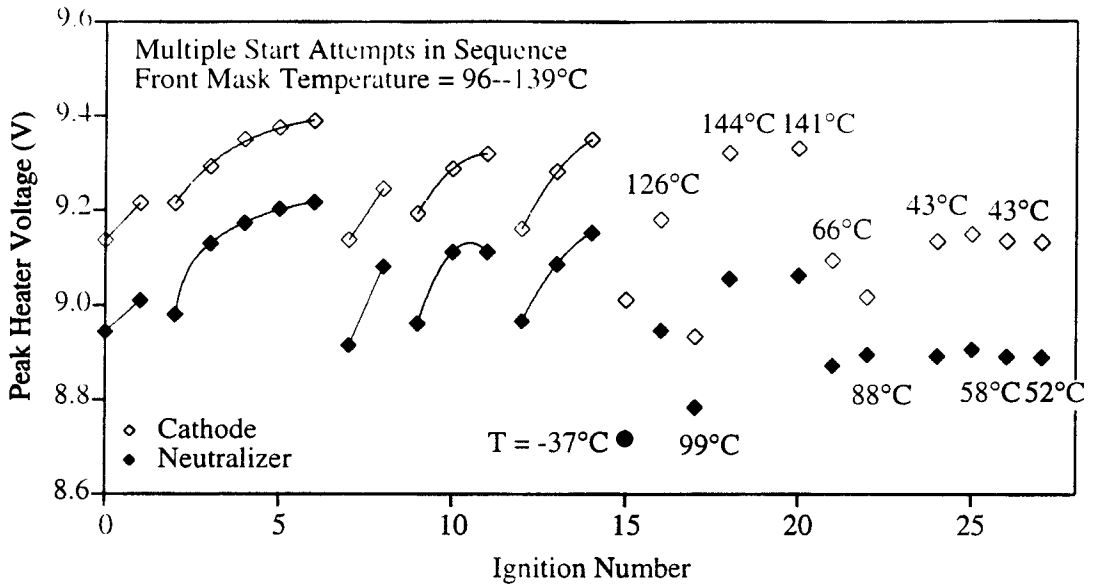

Figure 16: Time history of peak cathode and neutralizer heater voltages.

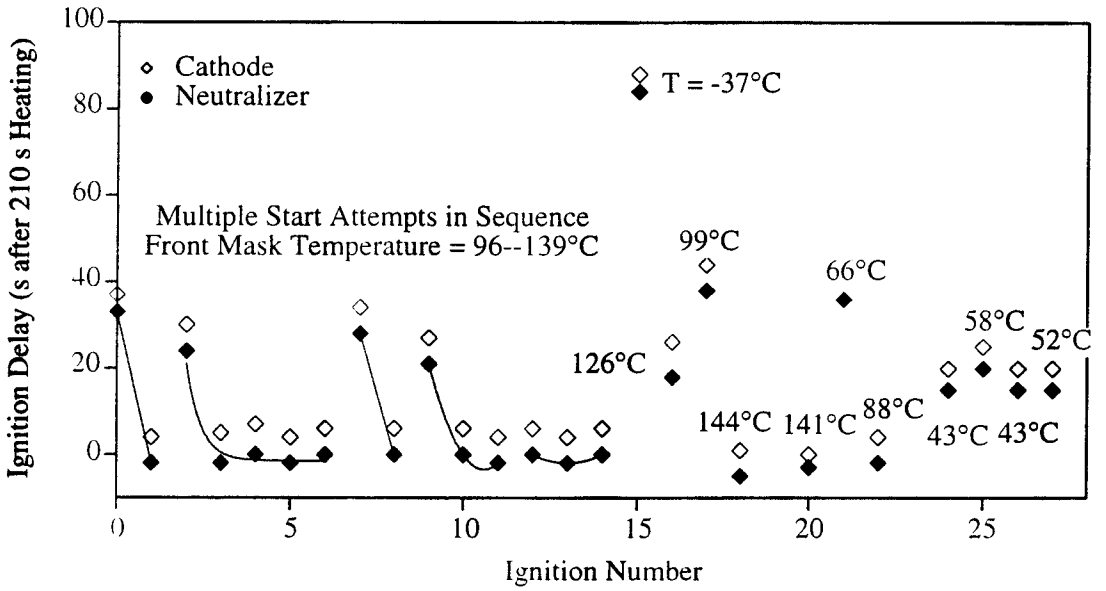

Figure 17: Time history of cathode and neutralizer ignition delays.

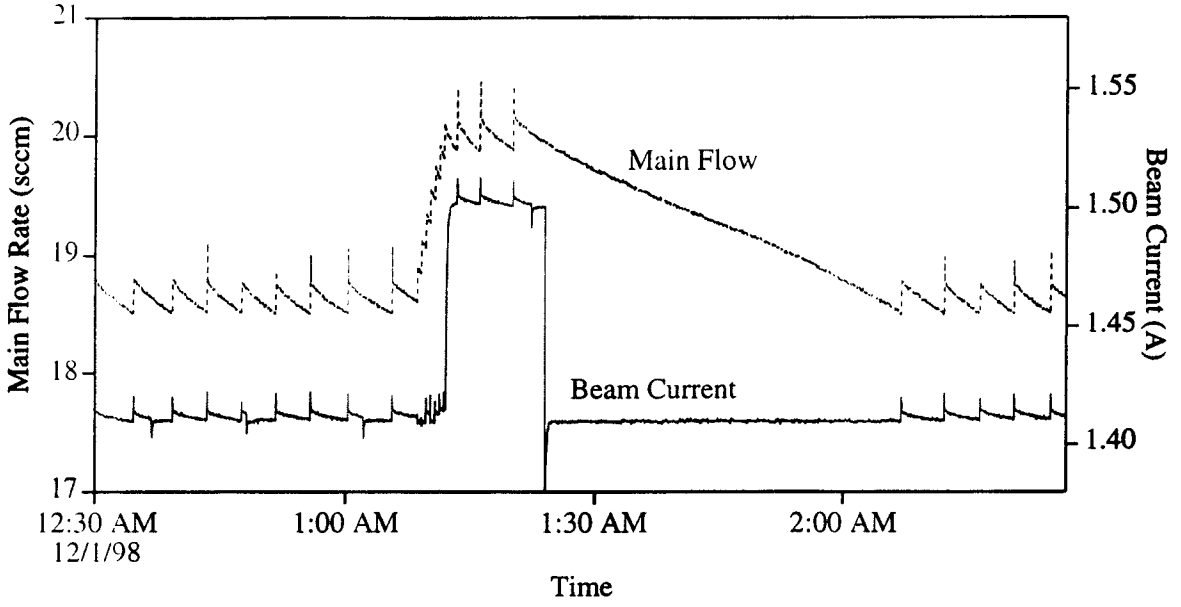

Figure 18: Example of throttle-up and throttle-down sequences.

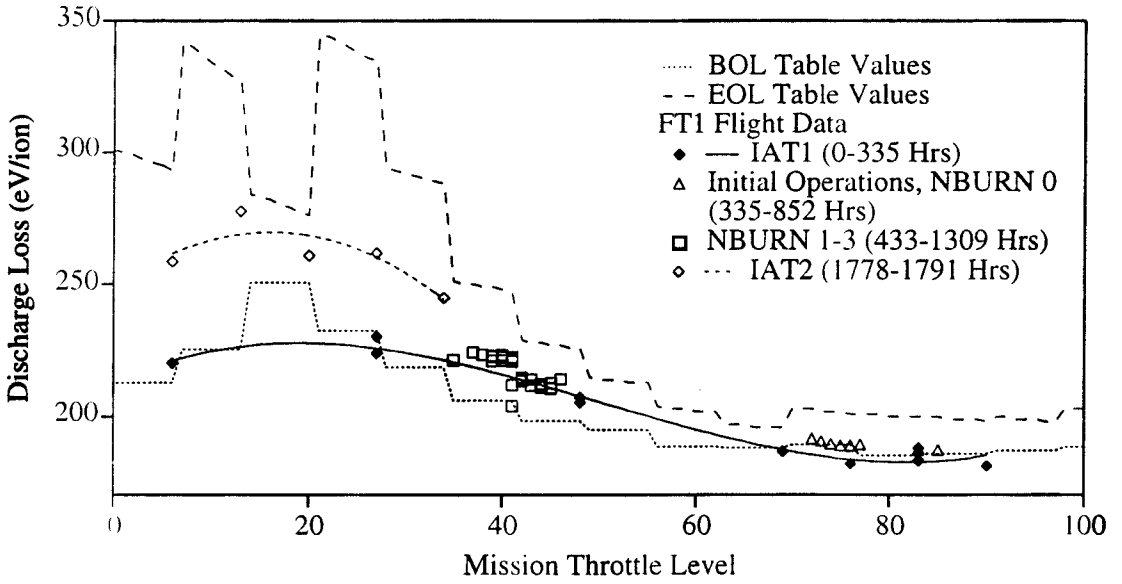

Figure 19: Discharge losses measured in flight compared to throttle table values.

NSTAR Throttle Level	Mission Throttle Level	PPU Input Power (kW)	Engine Input Power (kW)	Measured Thrust (mN)	Main Flow Rate (sccm)	Cathode Flow Rate (sccm)	Neutralizer Flow Rate (sccm)	Specific Impulse (s)	Total Efficiency
12	85	1.99	1.86	75.34	19.99	2.91	2.82	3035	0.602
11	83	1.94	1.82	72.55	18.63	2.75	2.67	3125	0.610
11	83	1.96	1.83	72.63	18.62	2.75	2.67	3131	0.609
10	77	1.84	1.72	69.54	18.59	2.75	2.67	3000	0.594
10	76	1.82	1.70	67.21	17.31	2.58	2.51	3109	0.602
10	75	1.79	1.68	66.81	17.33	2.58	2.51	3087	0.601
10	74	1.77	1.66	66.11	17.33	2.59	2.51	3054	0.595
10	73	1.75	1.65	65.64	17.31	2.59	2.51	3035	0.594
10	72	1.73	1.63	65.15	17.31	2.59	2.51	3012	0.592
9	69	1.67	1.57	62.27	16.08	2.50	2.43	3070	0.597
6	48	1.29	1.22	47.43	11.42	2.50	2.42	3006	0.573
6	48	1.29	1.22	47.39	11.44	2.49	2.42	3004	0.571
3	27	0.89	0.84	31.70	6.93	2.50	2.43	2770	0.511
0	6	0.50	0.48	20.77	6.05	2.50	2.43	1961	0.418

Table 4: Flight engine performance measured in space.

shown in figures (15) and (18). The IPS Manager software onboard the spacecraft is also designed to autonomously throttle the engine to track the peak power available from the array. The engine is initially throttled up until auxiliary battery power drain is observed, and then decreased until no battery power is required. Any time that battery operation is detected as the available array power drops or spacecraft power needs increase, the IPS is commanded to throttle down to accommodate the reduced power. This function was successfully demonstrated in all of the NBURNs, which were accomplished with no ground control over the detailed engine operation required.

Steady-State Setpoint Accuracy

As mentioned above, the flight flow rates are slightly higher than the throttle table setpoints. In addition, the beam current is 4–13 mA high over a range of 0.51 to 1.10 A. The beam current is controlled in flight to within ±2 mA by varying the discharge current in closed-loop. Variation in the beam current is driven primarily by the flow rate sawtooth, as shown in Fig. (18). The neutralizer keeper current is 17 mA low at the 2 A setpoint and 10 mA low at 1.5 A. The accelerator grid voltage is 2 V higher than the setpoint at all operating points. The beam voltage is on average about 3 V lower than the setpoints. The offsets in beam power supply settings result in slightly higher beam power levels than the throttling tables assume. This is largely offset by lower neutralizer power levels, as explained below. All of these parameters are well within the specified flight system tolerances.

Discharge Performance

As indicated in the previous section, the difference between the total engine power and the throttle table values is dominated by the discharge power difference. The discharge performance is summarized in terms of the ion energy cost plotted in Fig. (19). The standard error of these measurements is 1.5 percent. This plot shows the beginning- and end-of-life discharge loss as a function of mission throttle level. The data from early in the DS1 mission are quite close to the throttle table values except in the middle of the range (throttle levels 40-60), where the flight data are higher. This appeared to be true of the ground measurements as well, suggesting that the BOL throttle table discharge power is low by about 10 W in this range. The data from NBURNs 1–3 and IAT2 indicate that the discharge losses are increasing with time as a consequence of engine wear [9, 7]. The lowest throttle levels are particularly sensitive to engine wear and show the largest increases in flight, up to 40 W. All of the data are still bounded by the throttle

table BOL and EOL values, however.

The discharge voltage and current are compared with the throttle table values in figures (20) and (21). The voltages measured in flight are typically within 2 percent of the throttle table voltages. The ground test data are also plotted in this figure and tend to be slightly higher, although some of these measurements have not been corrected for voltage drops in the ground facility power cables. There is very little drift in the discharge voltage over the course of the flight, which is consistent with long duration ground test data [8, 7, 5]. The discharge current is also close to the BOL table values initially, with the exception of measurements at mission level 48. This is in the range where the table values appear to underestimate true BOL behavior. Unlike the voltage, the discharge current increases with time and drives the discharge power toward the EOL values.

Data on the sensitivity of discharge losses, voltage and current to small variations in flow rates and beam current from the on-going Extended Life Test were used to examine the effect of setpoint errors on the flight discharge parameters. The effects compete, and result in negligible changes in these parameters due to the small flow and beam current errors.

Ion Optics Performance

The ion optics appear to be performing very well so far in flight. The accelerator grid impingement current as a function of beam current is compared to ground test data in Fig. (22). The standard error of these measurements is about 0.03 mA. The data obtained in the ground test facilities are higher because they include a contribution from charge exchange reactions with residual tank gas. The flight impingement current levels in space are about 0.4 mA lower at 0.51 A and 1.7 mA lower at 1.5 A compared to preflight measurements in the JPL endurance test facility, which operates at pressure levels of $2\text{–}5\times10^{-4}$ Pa ($1.5\text{–}4\times10^{-6}$ Torr) over the full throttle range. Accelerator grid erosion measurements obtained in long duration tests in this facility are therefore conservative. Data obtained in VF 5 at NASA GRC, which has a residual gas pressure about 3 times lower than that at JPL, show impingement currents which are about 0.1 mA greater than the space values. The ratio of impingement current to beam current is shown as a function of beam current in Fig. (23). This parameter, which is used in some probabilistic models of accelerator grid erosion [15, 16, 17] ranges from 0.17 percent at 0.51 A to 0.28 percent at 1.5 A with a standard deviation of 0.012 percent.

A total of 88 high voltage faults have occurred during 1791 hours of engine operation (excluding those that occurred as a result of the initial grid short). There has been no evidence of electron backstreaming. The discharge loss has consistently increased slightly when the accelerator grid voltage is raised from -250 V after ignition to the throttle setpoint, which is the nominal behavior. This transition is monitored for decreases in the discharge loss, which could signal the loss of electron backstreaming margin.

Neutralizer Performance

The neutralizer power consumption has been 4–7 W lower than the BOL throttle table values due to a lower neutralizer keeper voltage, shown in Fig. (24). This power savings roughly compensates for a higher beam power demand due to the beam current offset. The voltage dropped by about 0.5 V over several days before many of these data were taken in IAT1. The IAT1 data show that at that point in the mission the keeper voltage was up to 2 V less than the pre-test values. This difference is not yet understood. The voltage has continued to decrease with time, as the data from the initial operations and the NBURNS show. This behavior has been observed in ground tests [8, 7, 5] and is an indication of improving emitter surface conditions.

There is no instrumentation on the DS1 spacecraft that allows the true neutralizer coupling voltage to be easily determined. The voltage of neutralizer common with respect to the spacecraft ground is metered, and the behavior is shown in Fig. (25). To properly compare this with the ground measurements of coupling voltage, also shown in this plot, the spacecraft potential with respect to the ambient plasma must be known. It may be possible to estimate this from the onboard plasma diagnostics, but this analysis is not yet complete. It is interesting to note that the voltage variation with throttle level has the same slope as that of the coupling voltage in ground measurements and that the magnitude is decreasing with

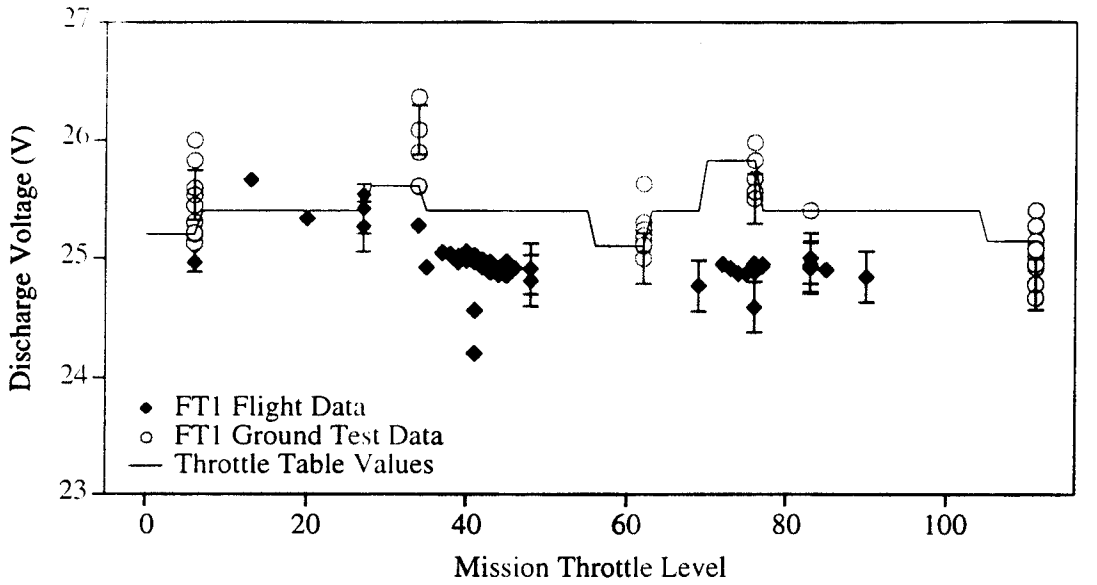

Figure 20: Discharge voltage measured in flight compared to throttle table and ground test measurements.

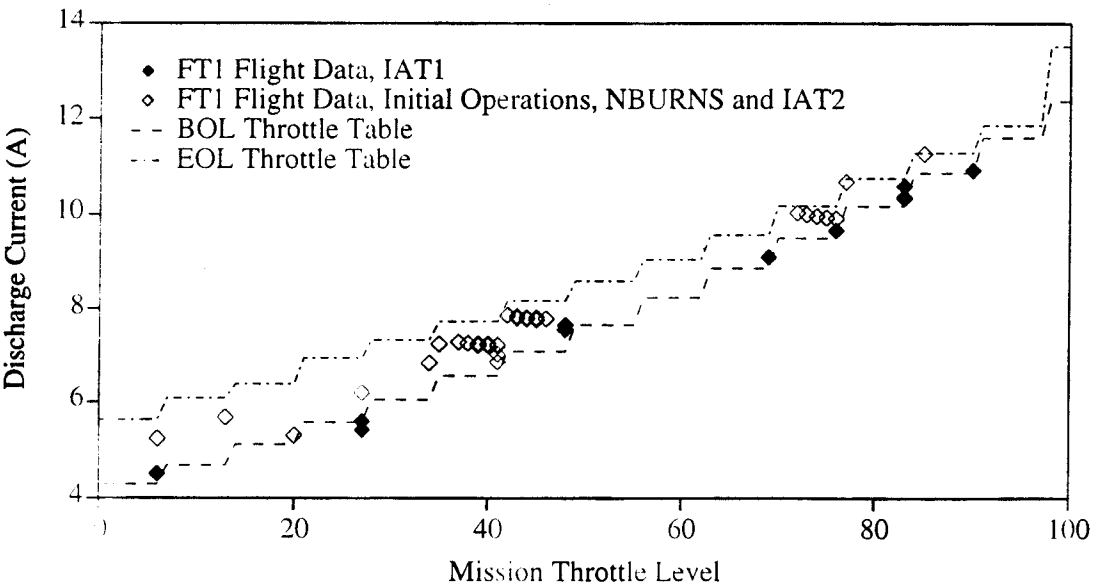

Figure 21: Discharge current measured in flight compared to throttle table values.

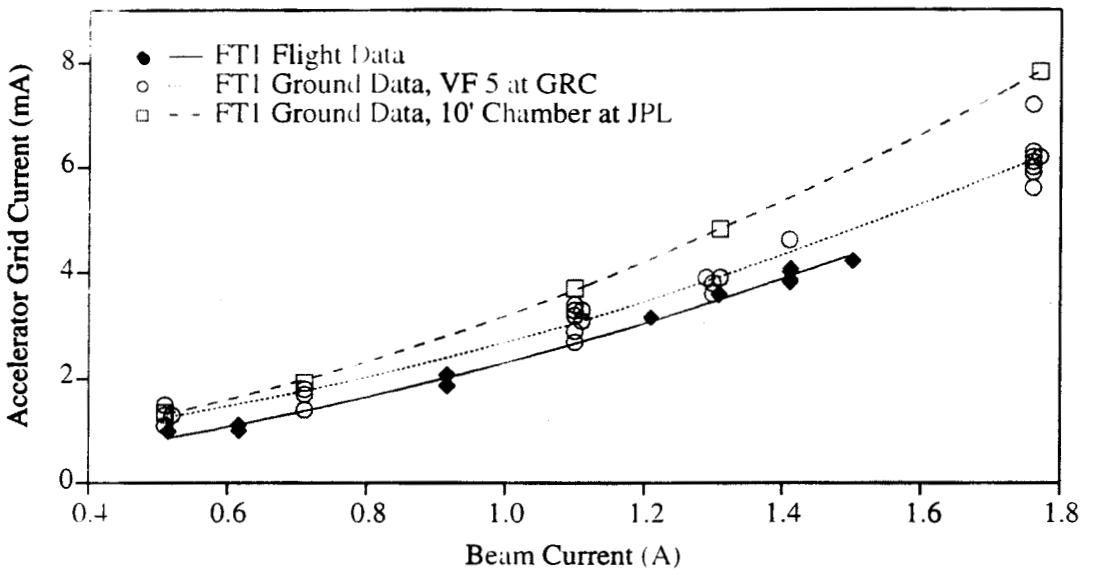

Figure 22: Accelerator grid impingement current measured in space compared to ground test measurements.

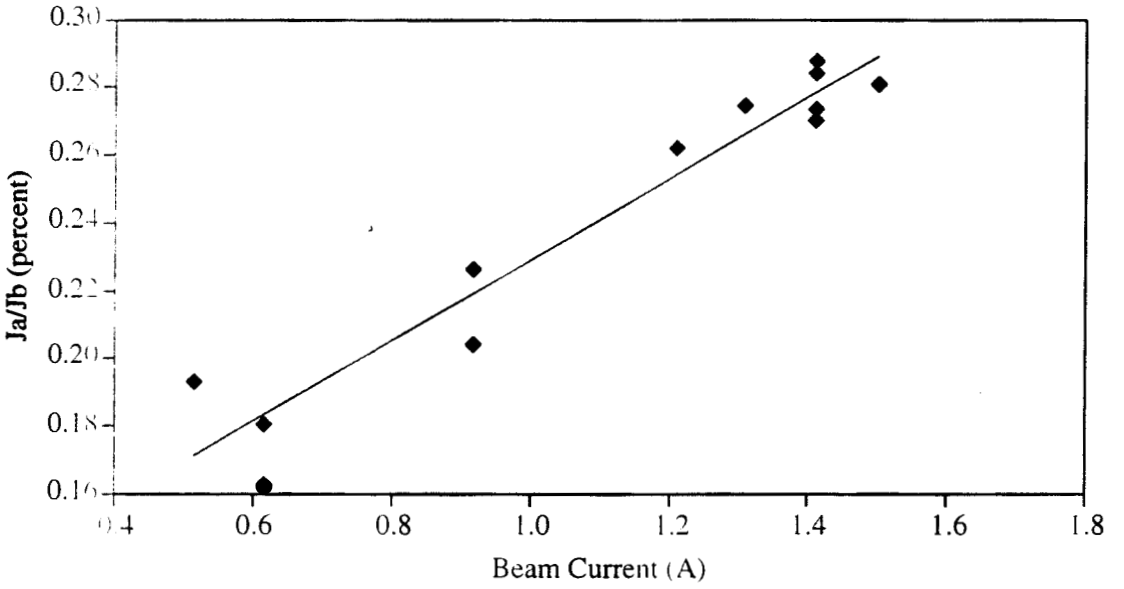

Figure 23: In-space ratio of accelerator grid impingement current to beam current.

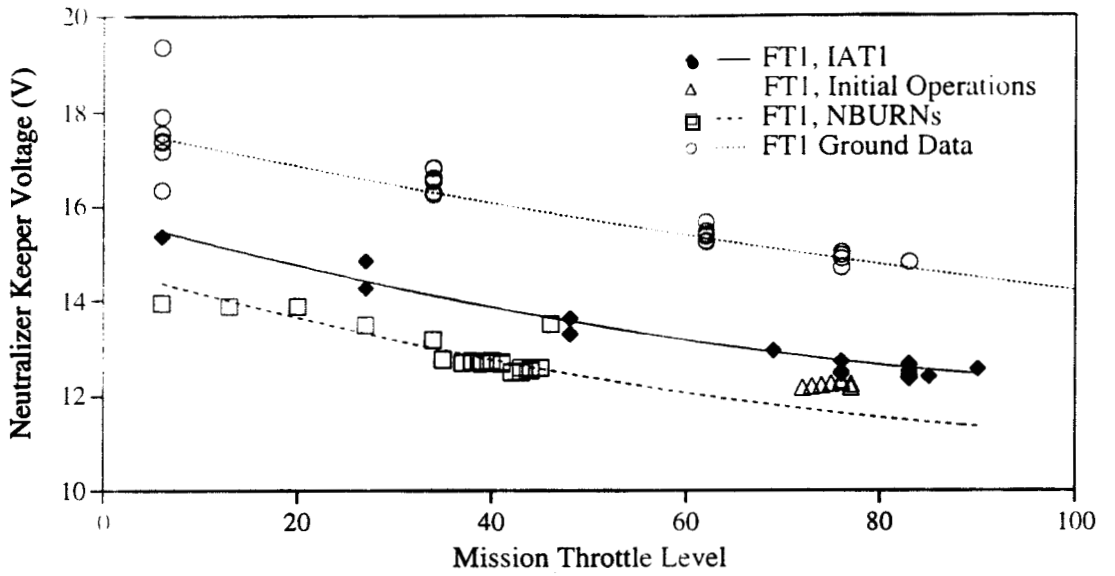

Figure 24: Neutralizer keeper voltage measured in space and in ground tests.

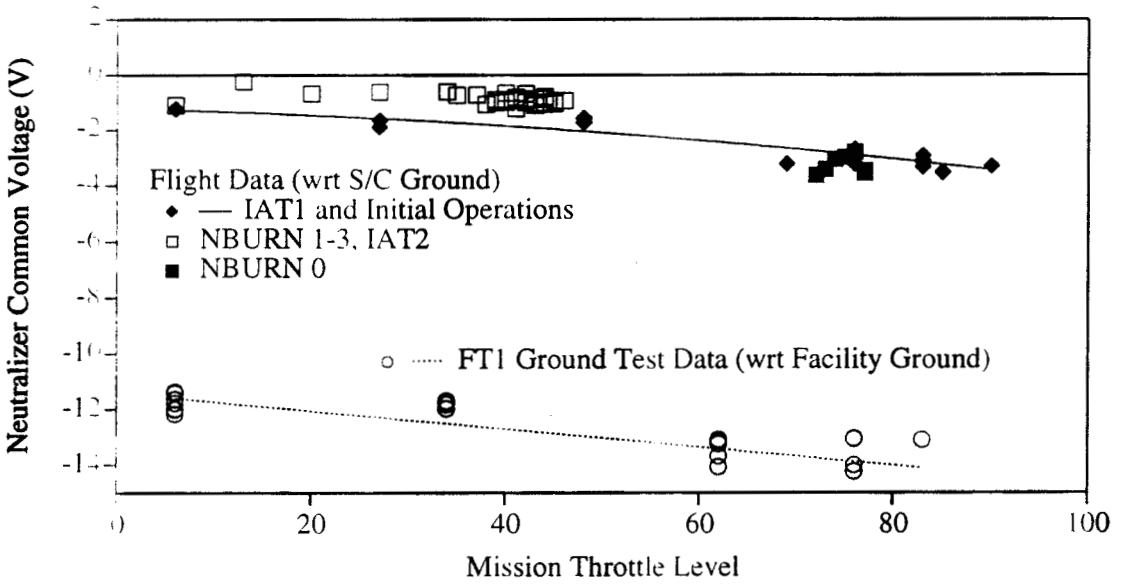

Figure 25 Neutralizer common voltage measured with respect to spacecraft ground in space and facility ground in ground tests.

time, whi also occurs in ground tests.

Mission Operations

Although e total thruster operating time so far has been ord of magnitude longer than that required by impul e propulsion systems, the mission operations de nds have been minimal. This is largely due to the uccessful implementation of a high degree of spacecr autonomy. Autonomous navigation has significant reduced the demands on the navigation and traje ory design teams and spacecraft control of the IP relieves the ground controllers considerably. In the initial phase of the mission a number of propul n engineers were involved in mission operations a validation. However, the final NBURNs have beco sufficiently routine at this point that not much wor orce is assigned to this area. The flight data diss ination and analysis has also been largely automate During Deep Space Network coverage the space ft telemetry is displayed in real-time on a website hat can be accessed by the flight team. Data are o stored in the JPL ground data system and auto tic queries to this system generate files of IPS da periodically that are sent via ftp to all flight tea members. A series of macros written in Igor Pro tware are used to automatically load, analyze and lot these data. The success in reducing mission o rations requirements with automation is an extrem significant result, because the fear of excessive op tions costs has been a major barrier to the accep ce of ion propulsion for planetary missions. It ow appears that the mission operations costs for P-driven spacecraft are similar to those for conve onal spacecraft or possibly less in cases where the se of ion propulsion results in shorter trip times.

Conclusions

The test ion propulsion on the Deep Space 1 primary mi n has been extremely successful so far. All norm IPS functions and some of the fault recovery m es have been demonstrated over a total of 1791 h rs of operation. The differences between system p rmance and engine operating characteristics in ce and in ground tests have been very small. T thrust appears to be slightly lower than the calcu d values at the higher power levels, and the PPU efficiency appears to be slightly higher than ground measurements. Fully autonomous navigation and operation of the IPS have also been demonstrated, achieving the goal of minimizing the required ground support for low thrust propulsion systems. This flight validates ion propulsion technology for use on future interplanetary spacecraft and has provided a wealth of information for future mission and spacecraft designers.

Acknowledgements

The authors would like to acknowledge the contributions of other NSTAR and DS1 Project members including Jack Stocky, Mike Marcucci, Dave Brinza, Mike Henry, Joe Wang, Walt Hoffman, Ken Fujii and Keith Goodfellow. We would like to thank Tim McElroy for analyzing the Doppler data to provide the in-flight thrust measurements. The research described in this paper was conducted at the Jet Propulsion Laboratory, California Institute of Technology, and was sponsored by the National Aeronautics and Space Administration.

References

[1] M.D. Rayman and D.H. Lehman. Deep Space 1: NASA's First Deep-Space Technology Validation Mission. In 48^{th} *International Astronautical Congress*, Turin, Italy, 1997. IAF-97-Q.5.05.

[2] G.B. Ganapathi and C.S. Engelbrecht. Post-Launch Performance Characterization of the Xenon Feed System on Deep Space One. In 35^{th} *Joint Propulsion Conference*, Los Angeles, CA, 1999. AIAA-99-2273.

[3] J.J. Wang et al. Deep Space One Investigations of Ion Propulsion Plasma Interactions: Overview and Initial Results. In 35^{th} *Joint Propulsion Conference*, Los Angeles, CA, 1999. AIAA-99-2971.

[4] J. S. Sovey et al. Development of an Ion Thruster and Power Processor for New Millenium's Deep Space 1 Mission. In 33^{rd} *Joint Propulsion Conference*, Seattle, WA, 1997. AIAA-97-2778.

[5] J.R. Anderson, K.D. Goodfellow, J.E. Polk, and R.F. Shotwell. The Results of an 8200 Hour

Wear Test of the NSTAR Ion Thruster. In 35^{th} *Joint Propulsion Conference*, Los Angeles, CA, 1999. AIAA-99-2857.

[6] J.A. Rawley. NSTAR Thruster Element Technical Requirements Document. Technical Report D-13[illegible], Jet Propulsion Laboratory, California Institute of Technology, Pasadena, CA. 1997.

[7] J.E. Polk, J.R. Anderson, J.R. Brophy, V.K. Rawlin, M.J. Patterson, and J.S. Sovey. The Results of an 8200 Hour Wear Test of the NSTAR Ion Thruster. In 35^{th} *Joint Propulsion Conference*, Los Angeles, CA, 1999. AIAA-99-2446.

[8] J.E. Polk et al. A 1000-Hour Wear Test of the NASA NSTAR Ion Thruster. In 32^{nd} *Joint Propulsion Conference*, Lake Buena Vista, FL, 1996. AIAA-96-2717.

[9] J.E. Polk, J.R. Anderson, J.R. Brophy, V.K. Rawlin, M.J. Patterson, and J.S. Sovey. The Effects of Engine Wear on Performance in the NSTAR 8000 Hour Ion Engine Endurance Test. In 3[illegible] *Joint Propulsion Conference*, Seattle, WA, 1997. AIAA-97-3387.

[10] M. Patterson, T. Haag, V. Rawlin, and M Kussmaul. NASA 30 cm Ion Thruster Development Status. In 30^{th} *Joint Propulsion Conference*, Indianapolis, 1994. AIAA-94-2849.

[11] K.D. Goodfellow, G.B. Gamapathi, and J.F. Stocker. An Experimental and Theoretical Analysis of the Grid Clearing Capability of the NSTAR Ion Propulsion System. In 35^{th} *Joint Propulsion Conference*, Los Angeles, CA, 1999. AIAA-99-2859.

[12] W.R. Kerslake and L.R. Ignaczak. SERT II 1980 Extended Flight Thruster Experiments. In 18^{th} *International Electric Propulsion Conference*, 1981. IEPC 81-665.

[13] J.E. Polk J.R. Anderson and J.R. Brophy. Behavior of the Thrust Vector in the NSTAR Ion Thruster. In 34^{rd} *Joint Propulsion Conference*, Cleveland, OH. 1998. AIAA-98-3940.

[14] V. Hruby, M. Patterson, and R. Becker. Thermal Environmental Testing of NSTAR Engineering Model Ion Thrusters. In 25^{th} *International Electric Propulsion Conference*, Cleveland, OH, 1997. IEPC 97-051.

[15] J.E. Polk, N.R. Moore, L.E. Newline, J.R. Brophy, and D.H. Ebbeler. Probabilistic Analysis of Ion Engine Accelerator Grid Life. In 23^{rd} *International Electric Propulsion Conference*, Seattle, WA, 1993. AIAA-93-176.

[16] J.R. Anderson, J.E. Polk, and J.R. Brophy. Service Life Assessment for Ion Engines. In 25^{th} *International Electric Propulsion Conference*, Cleveland, OH, 1997. IEPC 97-049.

[17] J.R. Brophy, C.E. Garner, J.E. Polk, and J. Weiss. The Ion Propulsion System on NASA's Space Technology 4/Champollion Comet Rendezvous Mission. In 35^{th} *Joint Propulsion Conference*, Los Angeles, CA. 1999. AIAA-99-2856.